Accelerators

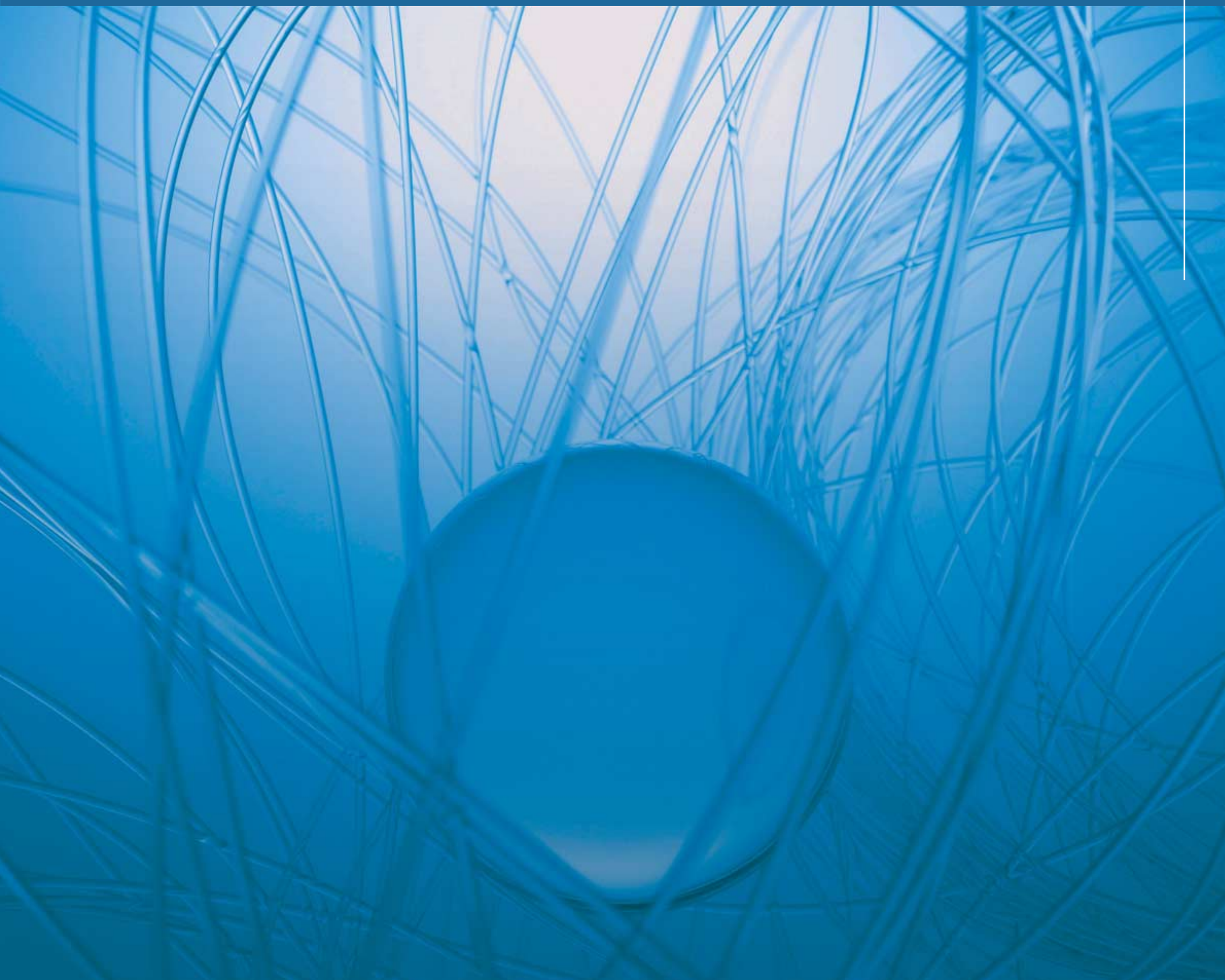

ACCELERATORS

1 Machine Operation

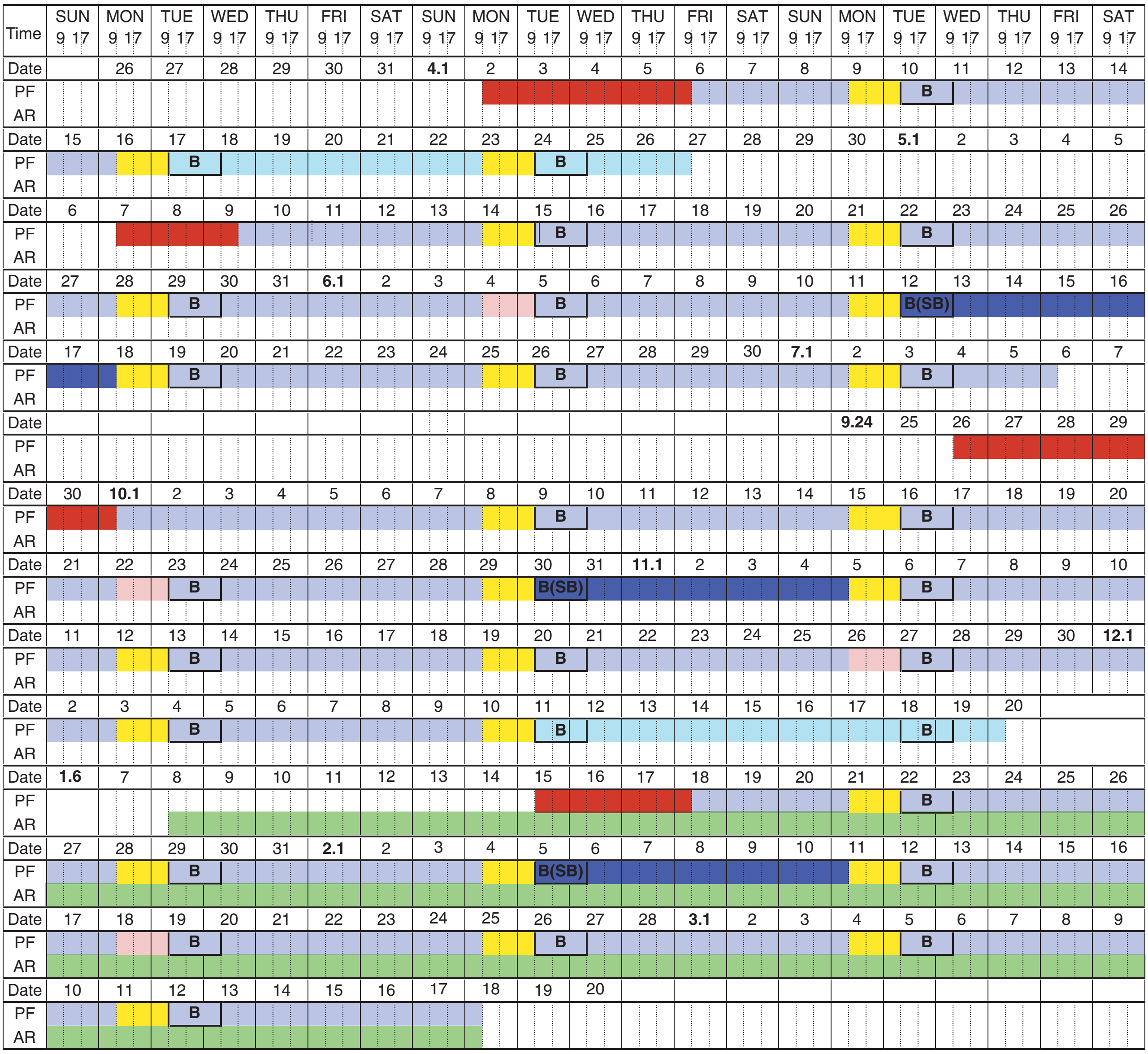

PF: PF Storage Ring

- Experiment using SR (2.5 GeV, 36 nmrad)
- Single bunch operation at 2.5 GeV
- Experiment using SR (3 GeV)
- Ring machine study
- Tuning and ring machine study
- Short maintenance and/or machine study
- **B** Bonus time during maintenance and/or machine study of injector linac

AR: PF-AR

- Tuning and ring machine study

Figure 1
Originally scheduled timetable of the machine operation in FY2001.

Summary of Machine Operation of the PF Storage Ring

Throughout 2001, the PF light source division staff continued efforts to maintain highly reliable operation, improve the performance of the PF Storage Ring, and undertake new developments.

Table 1 gives statistics of operation of the PF Storage Ring during fiscal year 2001. The bar graph in Fig. 2 shows the operation time, scheduled time and effective time since 1982. Total operation time of the PF Storage Ring was 5536 hours. Scheduled operation for multi-bunch was 4104 hours and 432 hours for single bunch mode. Net user time was 3974 hours and 413 hours for multi-bunch and single bunch mode, respectively. Thus, successive operation for users of the scheduled operation time was 96.8% for multi-bunch and 95.6% for single bunch. The product of beam current I and beam lifetime τ in 2001 is shown in Fig. 3 with those of the last five years. The values of $I\tau$ this year were about 1300 A min (21 A hr). We injected the electron beam into the ring at 9 a.m. every day, and the initial beam current was 450 mA. Figure 4 presents the average stored beam current between each injection, and the value for this fiscal year reaches almost 350mA. These results show that the PF Storage Ring operation is quite reliable with high current and long beam lifetime. Total failure time was 350 hours, and Fig. 5 gives the failure time (%) for scheduled operation and is about 1.3% through this year.

Although the failure time for machine operation was effectively low, we examined the causes of the failures and evaluated maintenance free time before failure (MFTBF). The failures which interest us include any failures causing beam dump, that is injection problems, RF reflection, problems with the RF power supply system. The failures include working of the interlock system of the ring control system, the insertion devices, and the radiation safety system. The failure also includes waiting time for the next injection from KEK-B linac after beam dump. The overall MFTBF of the PF Storage Ring is 112.9 hour, while it was 54.9 hour in the fiscal year 2000 operation. The contribution and effort of the light source staff had made this a fruitful this fiscal year.

Table1 Statistics of the PF Storage Ring Operation during FY 2001.

	Multi-bunch	Single-bunch	Total
Ring Operation Time (hours)	5104.0	432.0	5536.0
Scheduled user time (hours)	4104.0	432.0	4536.0
Net user time T (hours)	3973.5	413.2	4386.7
Time used for injection (hours)	59.5	17.8	77.3
Integrated current in T (A×hours)	1361.7	20.0	1381.7
Average current in T (mA)	342.7	48.3	--
Number of injections	190	54	244
Interval between injections (hours)	20.9	7.7	--

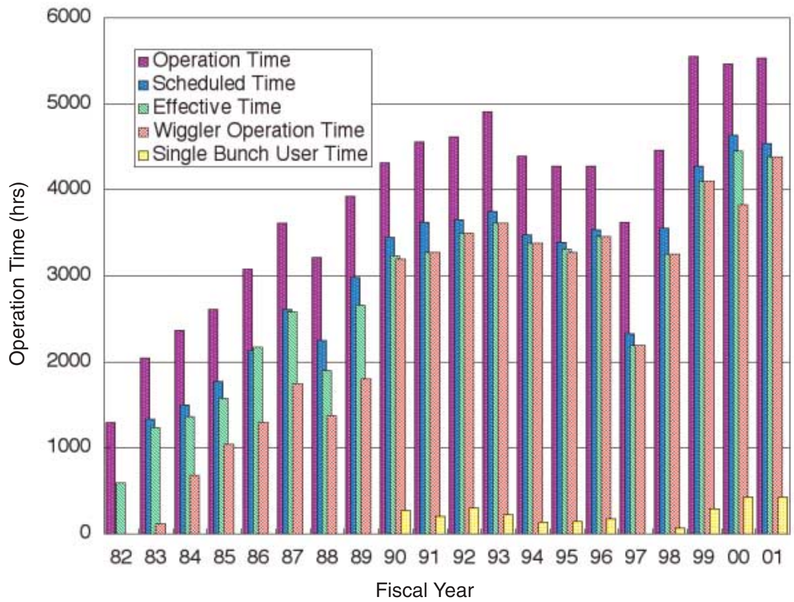

Figure 2
Operation time history of the PF Storage Ring.

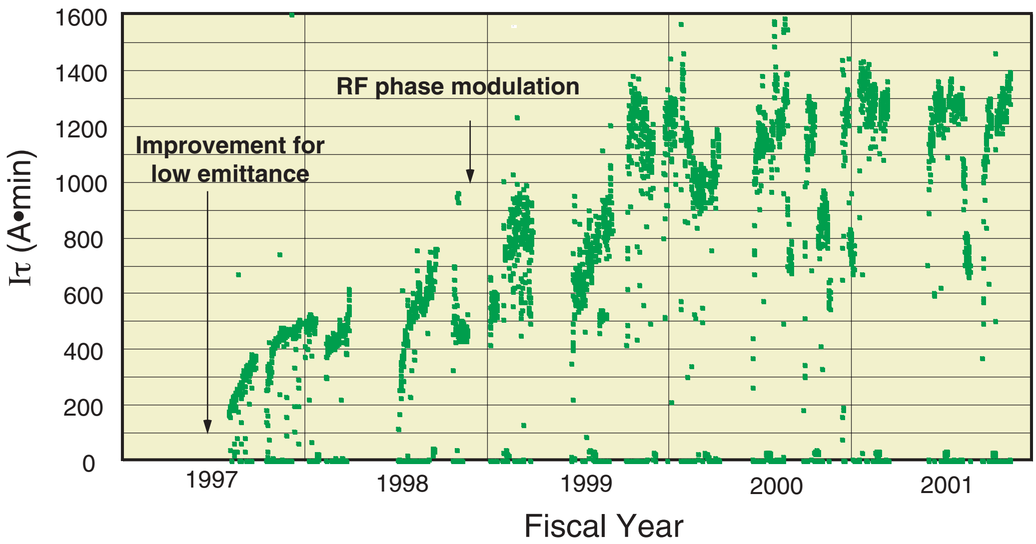

Figure 3
Iτ history of the PF Storage Ring in recent 5 years.

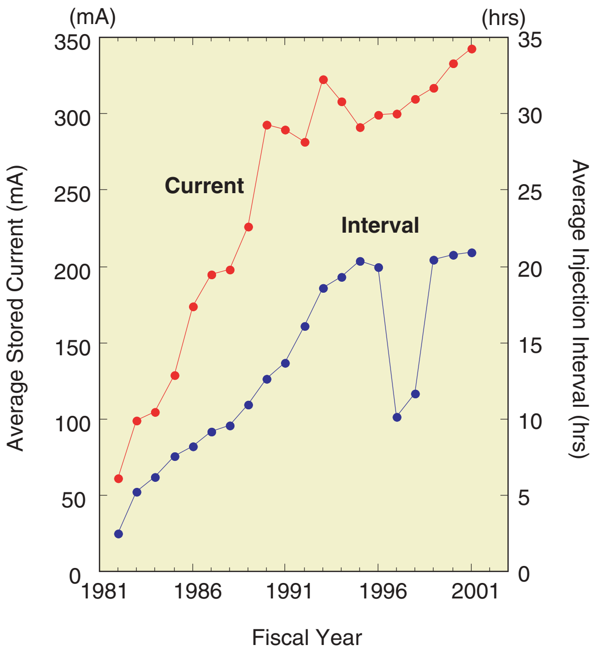

Figure 4
Average current and injection interval of the PF Storage Ring.

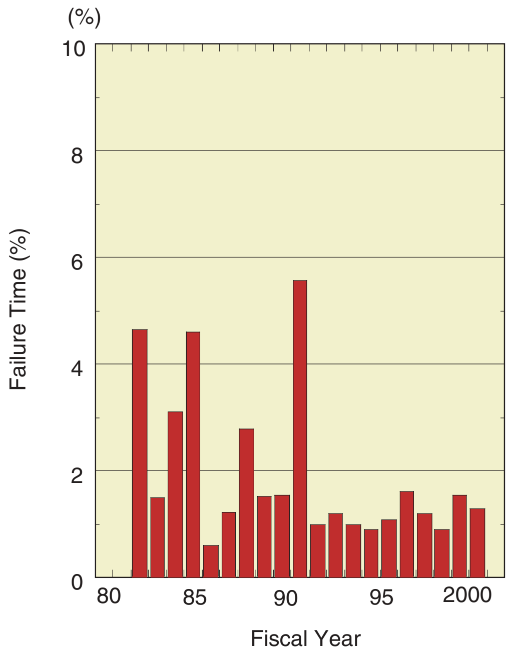

Figure 5
Failure time history of the PF Storage Ring.

Summary of Machine Operation of the PF-AR

As reported in the preceding Activity Report, IMSS had obtained a supplemental budget for the PF-AR upgrading from the government. We produced vacuum ducts made of OFHC copper, BPMs, steering magnets, and reinforced HOM dampers in APS cavities, and also replaced the PF-AR control system with a new one, that is, the EPICS system. All of these were installed, and the first beam was injected into the improved PF-AR on January 8, 2002. We continued commissioning the PF-AR systems for one week. The reason why the PF-AR commissioning time was so short is that KEK-B restart was already arranged for January 16. Through January to March we made efforts to tune-up the machine, especially to control COD and to confirm it by observing SR light in the beam lines. According to progress of the machine tuning, we could keep the initial stored beam current of 40 mA. New pumps (DIPs and Ti sublimation pumps) worked well, outgas caused by PSD reduced gradually by photon accumulation (integration of the stored beam current), and the ring pressures normalized by the stored beam current became 2×10^{-5} [Pa/A]. More detailed information on the commissioning is reported in next section. By the end of fiscal year 2001, we had operated the PF-AR for about 1416 hours. Opreation statistics of the PF-AR is shown in Table 3, and operation time in Fig. 6. The beam lifetime became beyond 700 minutes so injections were reduced to 6-7 times/day while they were 11-12 times/day in the previous PF-AR as is shown in Fig. 7.

As mentioned above, the PF-AR upgrading succeeded in both component production and ring commissioning. In the coming fiscal year we will try 3.0-GeV injection to obtain higher beam current without any beam instabilities, that is over 50 mA, and to reduce the beam emittance by phase advance of Q-magnets. We will also restart applications for coronary angiography.

Table 3 Operation statistics of the PF-AR in FY2001.

Operation Time	1416.0 h	100.0%
SR Experiment	353.0 h	24.9%
Beam Development	1010.0 h	71.3%
Failure	28.5 h	2.0%
Miscellaneous	24.0 h	1.7%

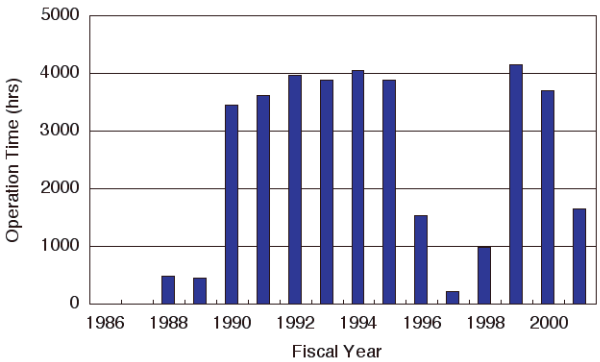

Figure 6
Operation time history of the PF-AR.

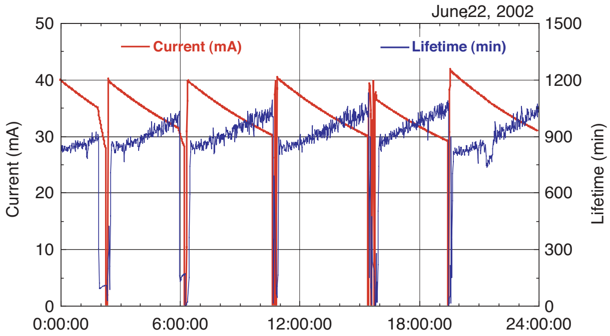

Figure 7
Typical one-day operation of the PF-AR.

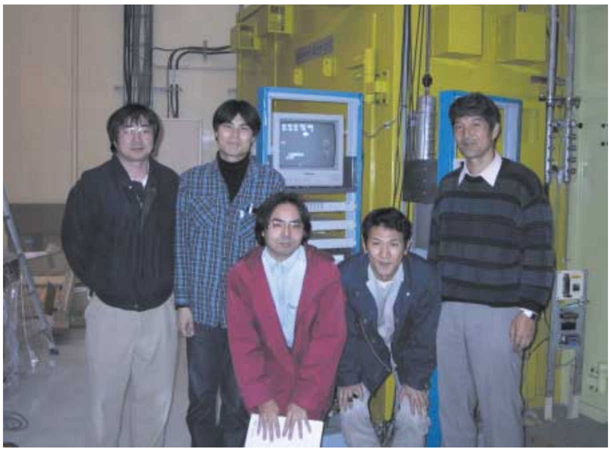

2 PF-AR Upgrading Project

2-1 General Description of the Upgrading Project

The PF-AR was originally constructed as a booster of the TRISTAN project, and had been partially used as an X-ray source. The ring was converted into a dedicated pulse X-ray source after completion of the project. However, because the ring was not designed as a dedicated light source, it has a lot of problems to be solved: short beam lifetime caused by insufficient vacuum system performance, low reliability due to superannuation of the machine components, imperfect closed orbit controlability due to lack of reliability of the beam position monitor (BPM) system, insufficient number of beamlines, the unsatisfactory beam current limited by the RF system, etc. In order to solve some of them, we decided to improve the vacuum system and the BPM system within the annual budget of KEK in the beginning of 1999, and began to manufacture the new vacuum ducts made of OFHC copper with newly designed BPM electrodes. In the mean time, the Government approved a supplementary budget for the PF-AR upgrading project in December 1999. The following are the main improvements based on the budget. Vertical steering magnets to improve the orbit control capability and quadrupole and sextupole magnets that were newly designed not to interfere with SR beamlines were manufactured. The power supplies for the steering magnets were all renewed and the power supplies for the new quadrupoles were newly manufactured. The remote control system of these power supplies including the old supplies for the bending and quadrupole magnets was completely renewed. The central control system of the light source was changed from the old NORDAL system to the EPICS that is successfully used in the KEKB control system. The radiation safety that secures safety of users in the experimental halls was also renewed to improve its reliability. Since the budget was limited, we decided to reuse the old injection system including the injection beam transport line and the APS acceleration cavities with the reinforced higher-order-mode loads.

The routine operation of the PF-AR came to an end in the end of February 2001 previous to the start of the upgrading work. The north-west experimental hall for new beamlines was constructed and an in-vacuum-type insertion device that will provide SR for a new beamline in it was designed and manufactured. In order to keep the radiation level around the injection point and in the south experimental hall as low as possible, the injection septum magnets were shielded and new shielding walls and ceiling were constructed in the hall. New components including an insertion device that had been made and delivered by the last fiscal year were installed in the ring and the magnet system was precisely surveyed and finely aligned. These works were nearly brought to completion by the end of December 2001. We started the commissioning of the light source exclusively using the injector linac from January 8, 2002. We succeeded in finding machine parameters with which electrons were smoothly injected at 2.5 GeV and accelerated up to 6.5 GeV within a week that was allotted to us in the tight schedule of the electron accelerator complex including the 2.5-GeV PF Storage Ring and the KEKB. We began the beam scrubbing to improve the vacuum pressure and the search for the optimum operating conditions from the middle of January. We have fixed standard machine parameters by the end of March 2002 to the routine operation for users that is scheduled to start from the beginning of April 2002.

2-2 Commissioning

Commissioning for the PF-AR was started on January 8, 2002. Since the operation time of the PF Storage Ring and the KEKB that shared the injector linac with the PF-AR had been scheduled to start on January 15 and 16, respectively, all the commissioning works should have been completed within one week. In order to make the commissioning work smooth, we decided to start the operation with a set of machine parameters very similar to old one.

On the first day of the commissioning, after adjusting the injection orbit by utilizing a single pass beam position monitor, we confirmed the beam circulation of about 200 turns without RF. Next, we turned the RF acceleration system on, and we were able to store the beam with the current of 2 mA at 2.5 GeV.

On the second day, we finely tuned the new BPM system and the betatron tune measurement system using the stored beam, and these were successfully commissioned. The closed orbit could be measured with greatly improved accuracy. After we adjusted the ring energy and corrected the choromaticity, the stored beam current could be over 10 mA at 2.5 GeV.

On the third day, the transverse feedback system was tuned and the octupole magnets were excited. As a result, the stored beam current reached 17 mA at 2.5 GeV.

On the fourth day, we finely adjusted the tracking for the power supplies of quadrupole and bending magnets to ramp up the energy from 2.5 GeV to 6.5 GeV.

After 3 days, the stored beam current reached 25 mA at 6.5 GeV, and the vacuum conditioning through the SR irradiation at 6.5 GeV was started. The history of the stored beam current and the vacuum conditioning during the commissioning are shown in Fig. 1 and Fig. 2, respectively.

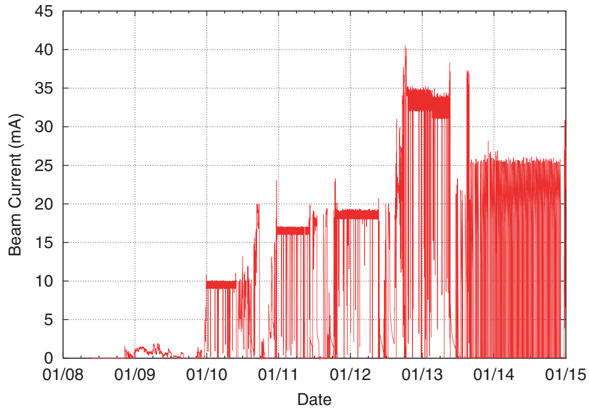

Figure 1
History of the stored beam current.

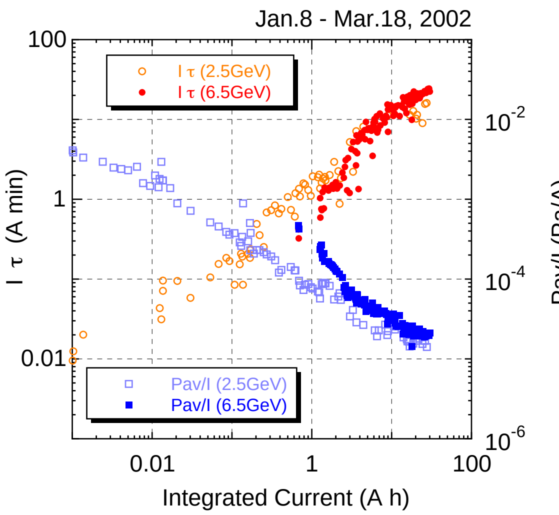

Figure 2
History of the vacuum conditioning during the commissioning.

After these machine tuning and machine studies (study of longitudinal feedback system, correction of the injection orbit and the beam optics correction, etc.), the stored beam current reached 42 mA at 6.5 GeV and the beam lifetime reached 500 min at the initial current of 42 mA.

The users operation will be re-started on April 16, 2002 with an emittance of 280 nm-rad.

2-3 Magnet System

We did not change the lattice configuration basically in the upgrade project. Thus, all existing bending magnets, most quadrupole and sextupole magnets, and their power supplies were reused. However, a few quadrupole and sextupole magnets were newly manufactured to avoid interference with both the existing and future X-ray beamlines [1]. The arrangement of the new magnets is shown in Fig. 3.

The vertical steering magnets were newly designed to ensure space for the pumping ports of the vacuum system, and the number of the magnets was increased from 44 to 79 for further orbit stabilization. Also, the power supplies for the steering magnets in both horizontal and vertical direction were replaced by new ones to improve not only the resolution but also the reliability.

The interfaces of all power supplies were exchanged from CAMAC to ARCNet, which was connected to EPICS.

In addition, the four octupole magnets were installed in the PF-AR to reduce the beam instability.

In February 2001, new quadrupole and sextupole magnets were installed in the PF-AR. The back-leg coil for horizontal steering, the interlock cables and the cooling water rubber hose were elaborately maintained by exchanging with new parts, as much as possible.

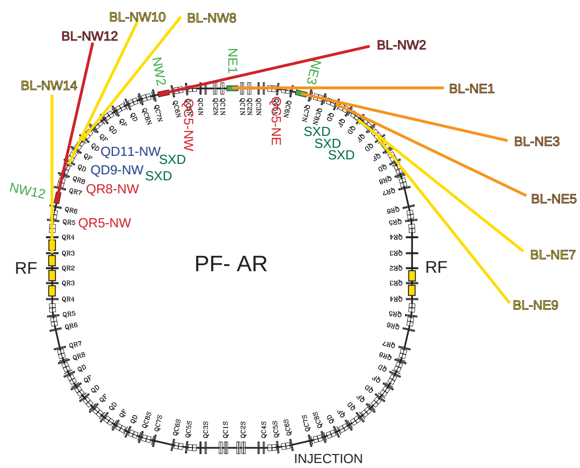

Figure 3
Arrangement of the new quadrupole and sextupole magnets.

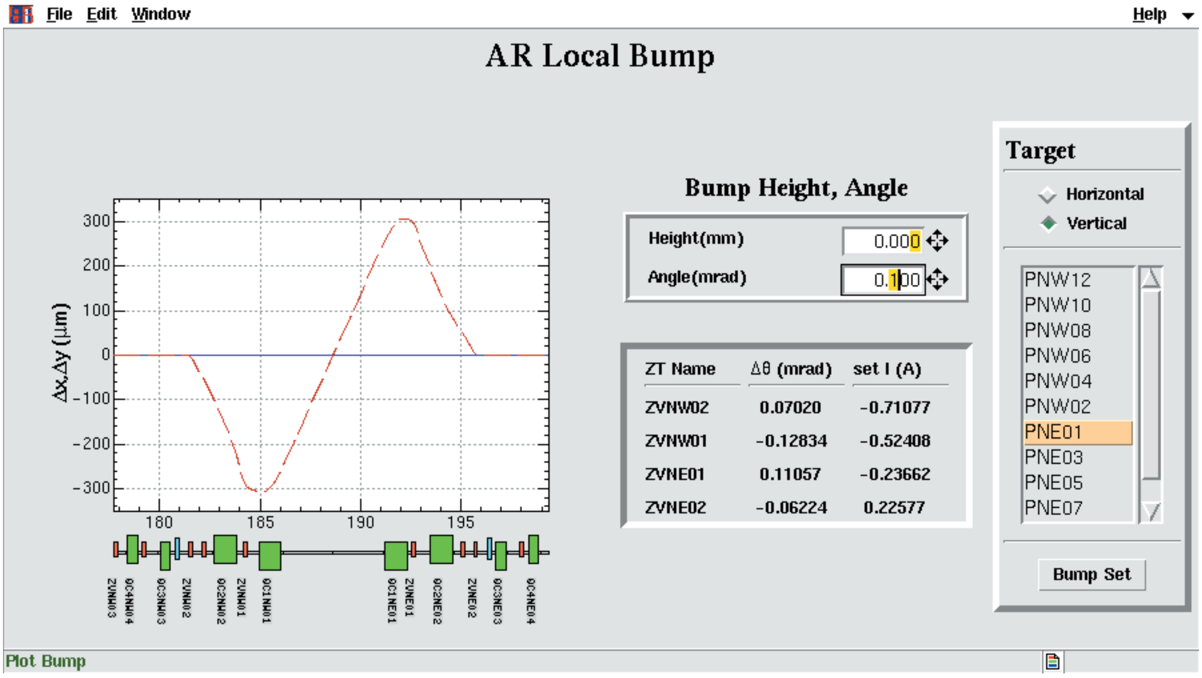

Figure 4
Example of control panel (Local Bump Set Panel).

Before the old vacuum system was removed, a survey and alignment of the bending and quadrupole magnets were carried out.

In parallel to the upgrade works for the ring, the new North-West Experimental Hall had been constructed. Since soil was removed in the construction, the ring tunnel was deformed. Therefore, we carried out the survey and alignment again at the end of December 2001 after the construction had been nearly completed.

The magnet control system was constructed by EPICS. The user interface consists of the power supply control system, the tracking control system and the beam optics correction system was programmed using Python and SAD/TKinter Script. An example of the magnet control panel (Local Bump Set Panel) is shown in Fig. 4.

[1] T. Miyajima *et al*.: "Field measurements of new magnets for the PF-AR upgrade project" *Proc. of Second Asian Particle Accelerator Conference, Beijing, China* (2001).

2-4 RF System

The high beam energy (6.5 GeV) of the PF-AR requires a large-scale rf system for beam acceleration. There are two (east and west) rf stations. Each rf station is comprised of a 1-MW klystron, an rf distribution network, a low-level system, and rf cavities. Two and four 11-cell cavities are housed in the east and the west rf sections, respectively. These cavities can provide an rf voltage of about 17 MV. After the upgrade of the PF-AR, we anticipate to increase the beam current up to 70 mA, which is about 1.7 times the beam current so far. This requires a total rf power of about 1.13 MW.

To this end, we have made some improvements on the rf system. First, we reinforced the higher-order-mode (HOM) loads for the cavities. Each cavity of the PF-AR is equipped with twelve HOM couplers which can damp harmful higher order modes. Each HOM coupler was terminated by a 1-kW broadband dummy load. Because we expected higher HOM-power from these couplers after the upgrade, we replaced all 70 dummy loads to newly developed 3-kW ones. The heart of the new dummy load is some beryllium plates with resistive stripes; the beryllium plates are forced to contact with a water-cooled copper block. This indirect water-cooling structure fits our need that we should avoid any water leak in the ring tunnel. Figure 5 shows a picture of the new dummy loads as installed in the tunnel.

Higher beam currents require one to operate the

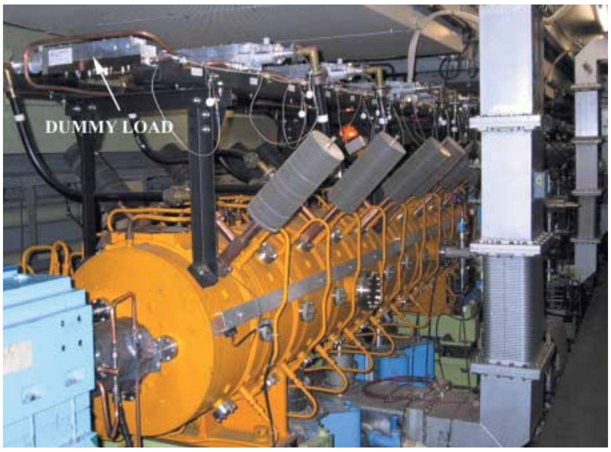

Figure 5
New higher-order-mode loads as installed on top of the cavities.

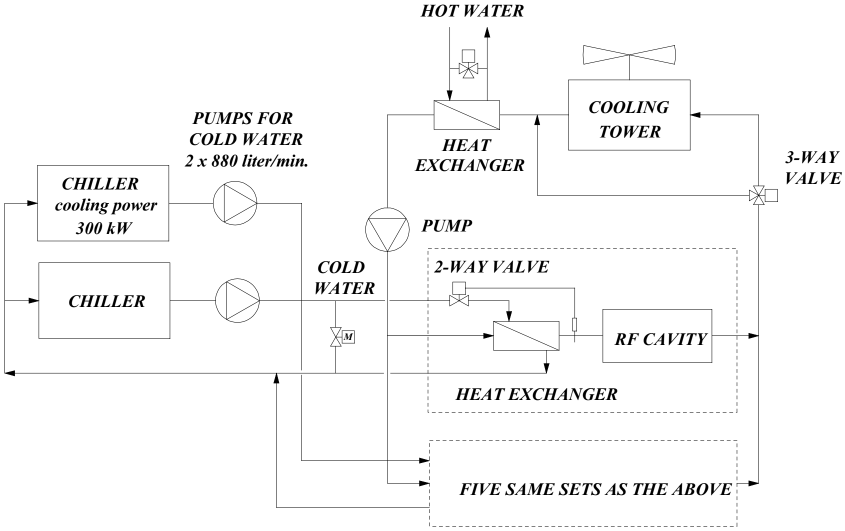

Figure 6
Temperature stabilization system for the cavity cooling water.

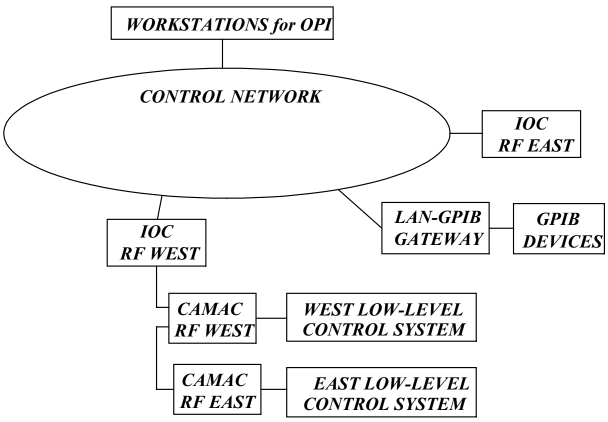

Figure 7
Outline of the rf control system.

klystron at higher (more than 80 kV) voltages. In these cases, the reliability of the crowbar circuit, which is used to protect the klystron under discharges, becomes very important. In order to achieve higher reliability, we improved the crowbar circuit so that all of the high-voltage components were placed in insulating oil. This should be very useful to prevent any corona discharge which may misfire the crowbar circuit.

In order to stabilize the cooling-water temperature for the cavities, a temperature stabilization system has been used. Figure 6 shows a block diagram of this system. It can stabilize the temperature of the cooling water by exchanging its heat with other cold water. We have prepared a remote control system, by which we can set the cooling-water temperature from the control room.

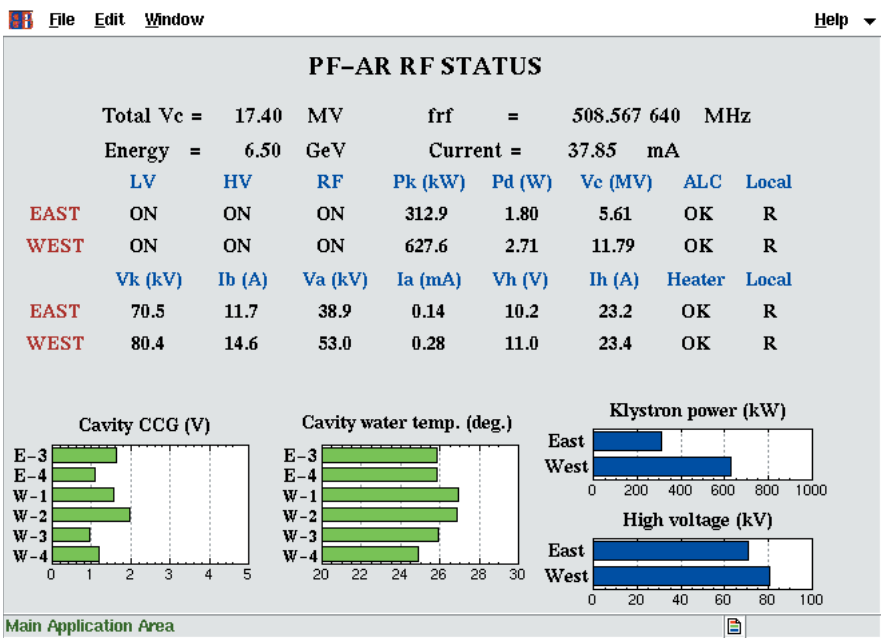

Figure 8
Control panel showing the operation status of the rf system.

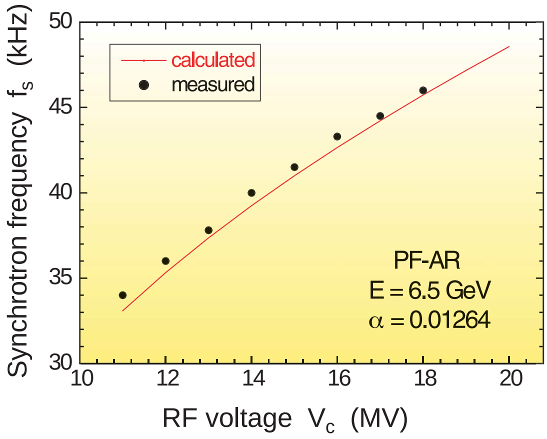

Figure 9
Measured and calculated synchrotron frequencies at full beam energy (6.5 GeV).

Figure 10
Thermal baking.

This function is useful for optimizing the cavity conditions under beam operations.

The rf control system was fully upgraded to an EPICS-based one. Figure 7 shows an outline of the new control system. Most of the equipments are controlled by an Input/Output Controller (IOC), which is connected to original CAMAC interfaces. We developed both an EPICS runtime database and operator-interface (OPI) programs. About 1200 database records were defined for the rf system. The OPI programs were written using both SAD/Tkinter script and Python/Tkinter language. Using this system, we can control all functions of the rf system. Figure 8 shows an example of the control panel which indicates the status of the rf system under operation.

After the upgrade, the rf system commissioned very smoothly. The measured synchrotron frequencies agreed well with the calculated ones, as shown in Fig. 9. At present, the maximum beam current under routine operations is about 40 mA. The present limitation comes from some collective effects such as coupled-bunch instabilities or other instabilities. According to the latest study, there is a good indication which shows the possibility of increasing the beam current by raising the injection energy from 2.5 to 3 GeV, and by optimizing other parameters.

2-5 Vacuum System

In the PF-AR upgrading project, the vacuum system was designed to meet the following requirements:

- Sufficiently low vacuum pressure (< 5×10^{-7} Pa) to realize the beam lifetime of more than 10 hours with a 6.0(6.5) GeV-100 mA beam stored
- Thermal tolerance of the photon absorbers for a 6.0(6.5) GeV-100 mA beam load
- Adaptability to some new devices, such as beam position monitors, steering magnets, insertion devices, and SR (Synchrotron Radiation) beamlines
- Unification of vacuum control system into the EPICS (Experimental Physics and Industrial Control System)

These requirements involved drastic replacement of almost the entire vacuum system, including beam chambers, vacuum pumps, vacuum gauges, a cooling water system, a compressed air system, and their control system.

Removal of old beam chambers and manufacture of new beam chambers were finished in FY2000. In FY2001, out-gassing process with thermal baking were performed on the beam chambers prior to the installation (Fig. 10), and the installation of all the new vacuum devices were carried out until December 2001. Special implement for installing the arc section chambers was necessary because they had to be inserted from outside the existing bending magnets under spatial restrictions.

The new beam chambers are equipped with water-cooling channels enough to absorb the maximum beam load and sufficiently large conductance to evacuate the PSD (photon-stimulated desorption) gas. 185 TSPs (Titanium Sublimation Pumps), 56 DIPs (Distributed Ion Pumps), and 36 SIPs (Sputter Ion Pumps) can provide total pumping speed of about 6×10^4 l/s. 81 CCGs (Cold Cathode Gauges) measure the vacuum pressure distribution along the ring and protect the vacuum devices from an unexpected vacuum accident by closing gate valves with interlock system. 175 RTDs (Resistance Temperature Detectors) always monitor the temperature of vacuum ducts. 72 WFDs (Water Flow Detectors) were installed to monitor the cooling water flow and to protect the beam chambers from an unexpected accident in the cooling water system. All of their controllers except for the RTD were replaced and the PLC (Programmable Logic Controller) was newly installed in the vacuum interlock system. These devices can be controlled and monitored remotely with the EPICS.

By the time the PF-AR commissioning started in January 2002, startup evacuation of the whole beam ducts were finished and the average pressure reached 3×10^{-7} Pa.

During the three-month commissioning period, vacuum ducts cleaning with the SR irradiation progressed smoothly (Fig. 2) and the beam life at 6.5-GeV operation grew up to 10 hours with a 40-mA stored current, which was about 4 times longer than the value of the old PF-AR. Although some problems, such as sudden lifetime drop phenomena, happened especially in the beginning of the operation, in general, the vacuum system started successfully.

2-6 Monitor System

The beam position monitor (BPM) system at the PF-AR has been partly upgraded. According to a replacing of the vacuum ducts, pickup units with feed-throughs are newly constructed. Total number of BPM pickup units is 90 (56 for normal-section part and 34 for straight-section part of the PF-AR). After the calibration of the electrical offsets, each BPM pickup unit is settled to an end of the quadrupole magnet. The fixed position of every BPM units are measured and recorded.

Mechanical coaxial relay switches had been used to switch the signals from four electrodes in the old BPM system. Because the lifetime of the mechanical relay switch is about 10^6 switchings, it has to be replaced every few months in order to measure the closed orbit distortion (COD) every 10 seconds. Coaxial switches with mercury relays were decided to be used due to their longer lifetime of about 10^9 switchings.

Many cables in the PF-AR tunnel are heavily damaged by the radiation. About 400 RF cables connecting between the electrodes and the switching relays were changed to new halogen-free radiation resistant coaxial cables. The switching relay control cables were also renewed only at the damaged end in the tunnel. The detector circuits and the data collection system are scheduled to be used as before.

After the commissioning of the BPM system, it could measure the beam orbit every 10 seconds during the machine operation, and supported commissioning of the machine. The new BPM system recovered its reliability and will contribute to the stabilization of the beam orbit.

For constructing a new beamline, NW12, in the upgrading project of the PF-AR, a pair of stripline pickup and transmission type kicker electrodes of the transverse feedback system were moved from the NW section to the SW section. Therefore, in the restart of the operation of the PF-AR, the parameters of the feedback system were adjusted. Figure 11 shows the observed resonance peaks to the horizontal tune with feedback off and on after the adjustment. With the feedback system on, the horizontal and vertical oscillations are suppressed below 10 dB. The damping time with the feedback system is 0.1 ms. This ability is almost same as with the one before the movement. With operation of the feedback system, a beam current above 10 mA can be stored.

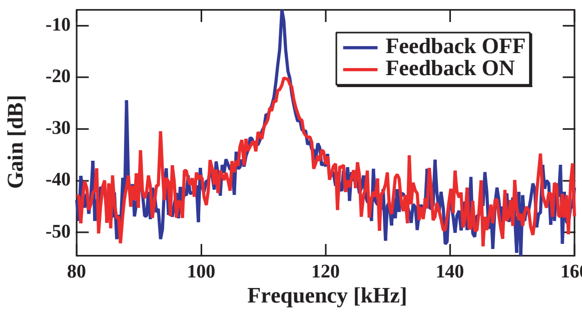

Figure 11
Observed horizontal tune spectra with the feedback off and on.

2-7 Control System

The design concept of the control system is based on the KEKB control system. Because the EPICS (Experimental Physics and Industrial Control System) was already working as a basic control system of KEKB, its experience was of great benefit for us in designing the PF-AR control system. Not only to minimize the load and the cost of the replacement, but the seamless operation between the LINAC and the KEKB was a point to be considered. The old control system based on HIDIC mini computer and NODAL software was replaced by the EPICS based control system.

We use several kinds of field busses such as CAMAC, RS232C, GPIB and ARCNET. The CAMAC crates and modules are used in many groups. Especially for the control of RF, BT (beam transport line) and beam monitor group, the existing serial highway which has a data-transmission rate of 2.5 Mbps, is fully used. ARCNET is used to control the magnet power supplies. The programmable logic controllers (PLCs) are used for the vacuum control system and for the accelerator safety system. Information from the PLCs are transferred to the EPICS IOC via RS232C. There are many GPIB instruments in the PF-AR. We use VME GPIB board and a LAN/GPIB gateway to control them.

The equipment control layer consists of VME Input/Output Controllers (IOC) locate at four sub-control buildings and main control room. A total of 11 IOCs are used for machine operation, and 2 IOCs for developments. We installed 64 MB memory in PowerPC-750 CPU board.

The specification of the UNIX server workstation for the PF-AR is listed below: 2 CPU, 440 MHz PA-8500 processor 1 GB memory, 36 GB system disk, external RAID disk 100 GB for data storage. For the modeling and simulations of accelerators, SAD cluster machines are also used.

There are eight personal computers (1GHz PentiumIII single CPU) for the operator consoles. We use five Linux machines with dual-head display board and use three Windows 2000 machines with four-head display. A dual PentiumIII machine for the WWW server is working, however, it can access from KEK internal machines for

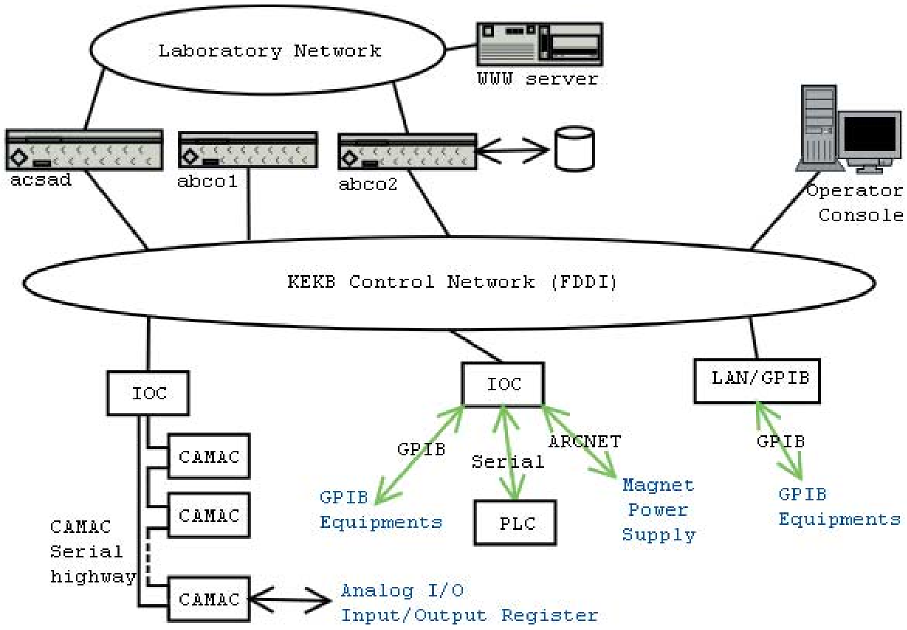

Figure 12
Schematic diagram of the control system.

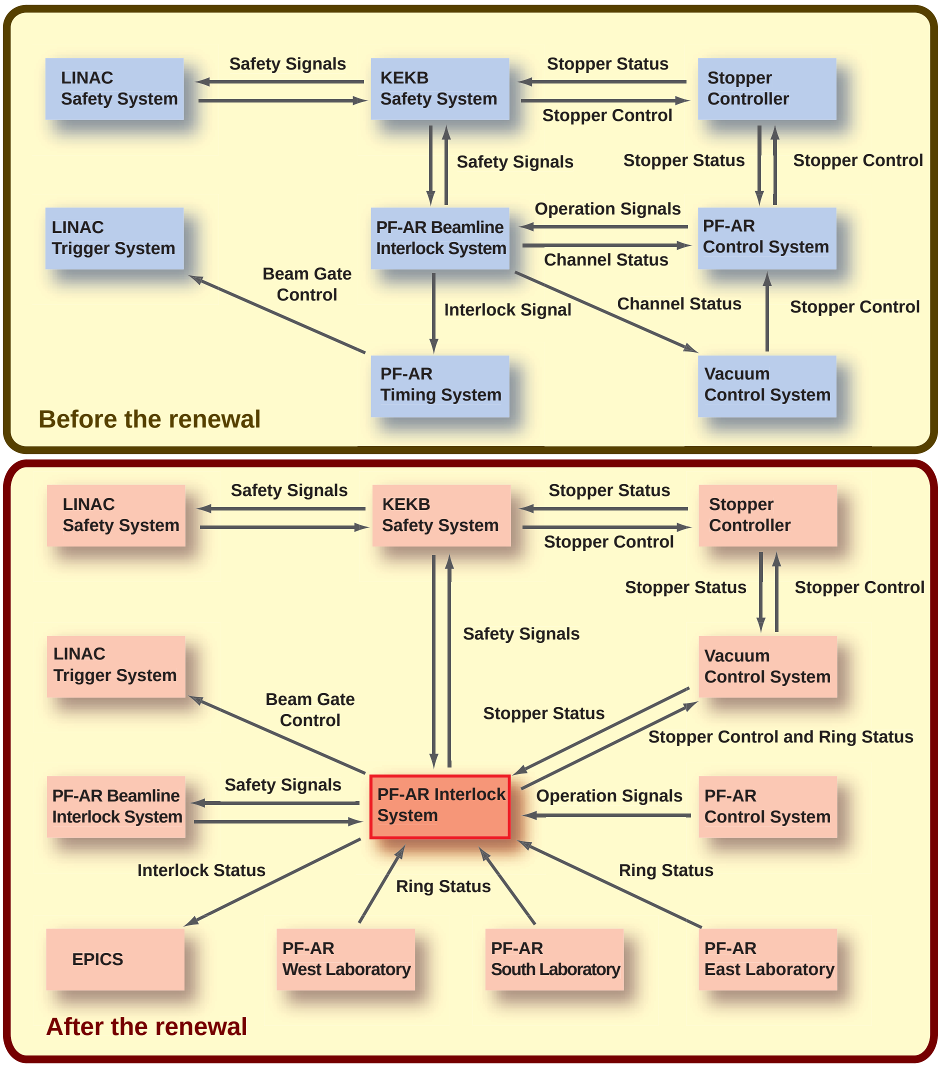

Figure 13
Accelerator safety system before (top) and after (bottom) the renewal.

now.

In order to develop the control software, many tools developed by EPICS community and KEKB control group are used. Especially for the operator consoles, MEDM (EPICS Display Editor/Display Manager), SAD/Tkinter and Python/Tkinter were mainly used. These software tools are very effective to create the control software. For the management of software versions, we used CVS (Concurrent Versions System) which is commonly used for that purpose.

Radiation safety system of the PF-AR is already controlled by KEKB safety system. We installed a new PLC to manage the safety signal among the beamline interlock system, accelerator control system and the KEKB safety system. The block diagram of the system is shown in Fig. 13. Most important role of the new PLC is to control the beam stopper and beam gate trigger depending on the status of accelerator. We carefully create the radder program of the PLC, and total system check were performed before the operation.

2-8 Insertion Devices

In FY2000 we had constructed an in-vacuum type undulator, U#NW2 which had a tilt mechanism of the magnet arrays. By using this mechanism we can realize two configurations of magnet arrays and switch them reversibly without any mechanical distortion in the support structure of U#NW2. They are: 1) a parallel (ordinary) configuration of the upper and lower magnet arrays and 2) a “tapered” configuration of the arrays with wider (closer) gap at one end of the undulator than at the other end. Corresponding to these configurations, we can realize two modes in the operation of U#NW2: 1) an

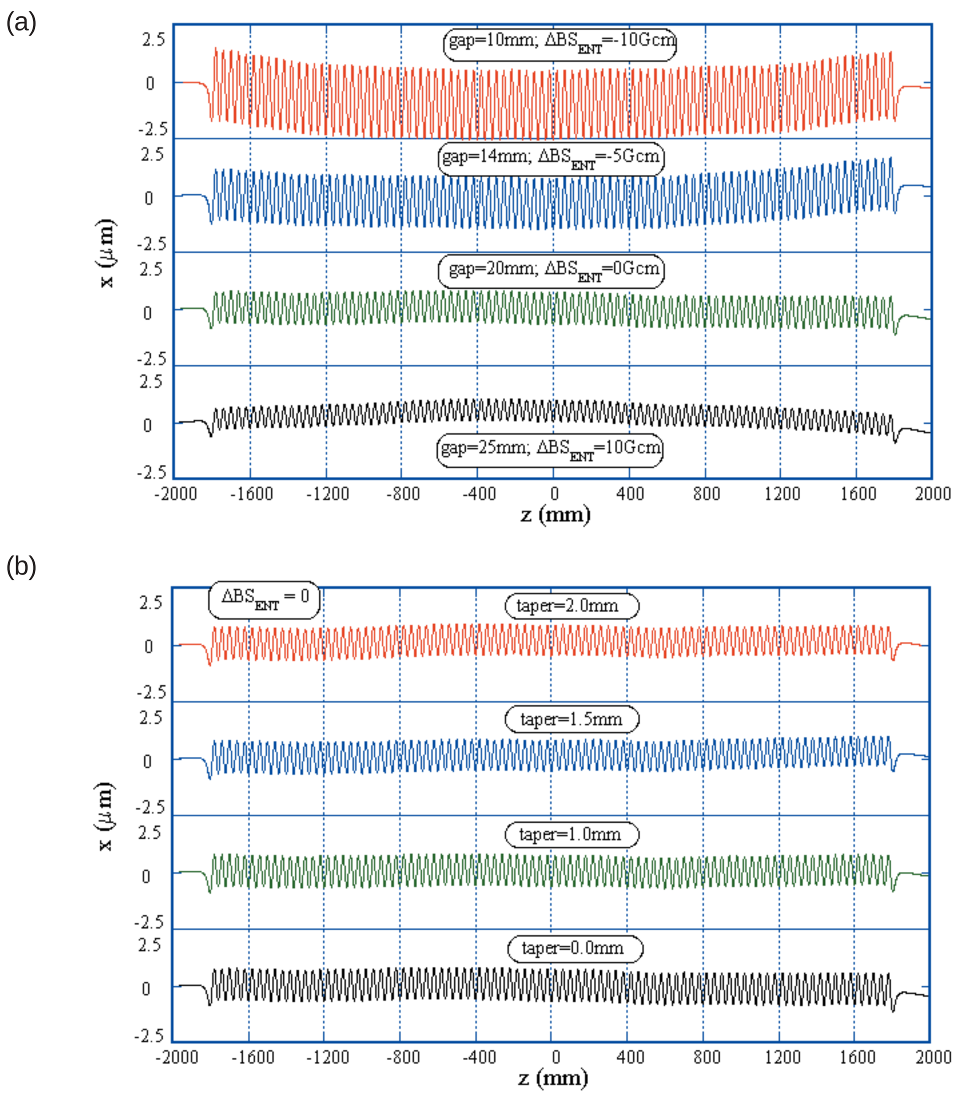

Figure 14
(a) Electron orbit in U#NW2 at several gaps at PF-AR’s operation energy of 6.5 GeV, which are calculated based on the precise measurement of the undulator field.
(b) Electron orbit in U#NW2 at a gap of 20 mm when we take the tapered configuration of the magnet arrays. The amounts of the taper are given as a difference of the gaps between at the entrance and at the exit of the undulator.

ordinary mode for high brilliance for precise diffraction experiments, and 2) a tapered mode for relatively wide bandwidth (some 10% as relative bandwidth) for the dispersive XAFS experiments. At the 6.5-GeV operation of the PF-AR, a spectral range from 5 to 25 keV is available with the lower harmonics (up to the fifth).

During FY2001 we have installed U#NW2 into the PF-AR as an X-ray source for the beamline NW2 after the precise adjustment of the undulator field and the vacuum commissioning. Figure 14 shows the result of the magnetic adjustment in terms of the electron orbit in U#NW2. We find that the state of the undulator field is kept good although the gap is changed at the ordinary mode (Fig. 14(a)), where ΔBS_{ENT} is errors in the kick which takes place at the undulator entrance (the values are increments compared to that at gap=20 mm). It should be noted that the undulator field is still kept good without any changes in ΔBS_{ENT} (Fig. 14(b)) when we take the tapered configuration. Calculated spectra corresponding to the tapered mode are given in Fig. 15. The calculation was made on the measured undulator field shown in Fig. 14(b) with the direct Fourier transformation with the parameters given in Fig. 15.

The vacuum chamber which contains all the magnets is evacuated by nonevaporable getter (NEG) pumps having a pumping speed of 4000 l/s and sputter ion pumps having a total speed of 240 l/s. The inside view of the chamber is shown in Fig. 16. Vacuum sealing on the surface of the magnets (period length of 4 cm and number of periods of 90) are made by TiN coating (5-µm thick). Bake-out for the whole vacuum system was made at 120°C for 48 hrs. so that we got ultra-high vacuum of 1.5×10^{-10} Torr. In order to avoid high-temperature deterioration of the magnets at the bake-out process, the magnets were prebaked at 145°C after magnetization.

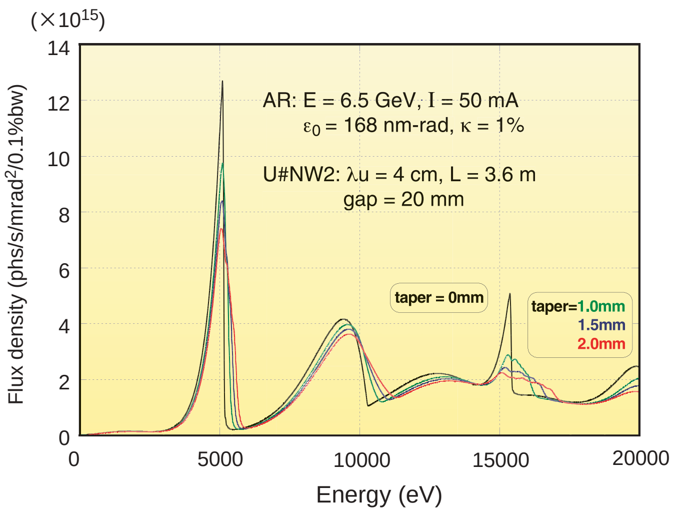

Figure 15
Calculated spectra for the tapered mode are compared to that for the ordinary mode. The calculation is made on the basis of the measured magnetic field shown in Fig. 14(b).

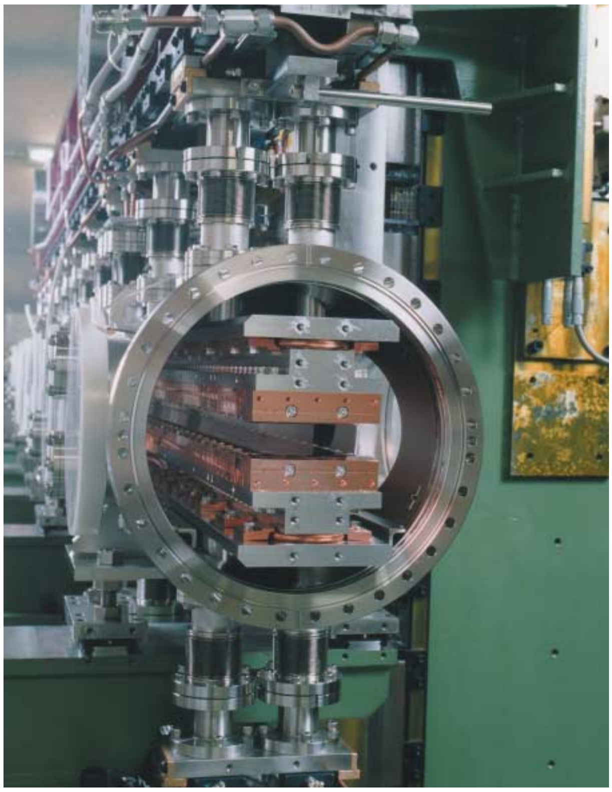

Figure 16
Inside view of the in-vacuum undulator, U#NW2.

3 Research and Developments at the PF Storage Ring

3-1 Upgrade of the Straight Sections at the PF Storage Ring

We have proposed the upgrade plan of the straight sections, where the insertion devises, RF cavities and injection system are installed. The upgrade is realized by placing new quadrupole magnets with shorter length and higher field gradient closer to neighboring bending magnets. In addition, the vacuum ducts and the front end of beam lines are replaced to avoid an interference with the magnets. Figure 1 shows the present and upgraded lattice configurations. As a result, four short straight sections of about 1.5 m are newly created. Furthermore, two long straight sections of 5 m are extended in those of about 9 m, and other sections are also extended. The optical functions are shown in Fig. 2. The beam parameters are almost the same as present ones. However, the longer undulators with planar or helical magnet configurations and mini-pole undulators with a narrower gap at a short straight section may be installed due to the upgrade. Figure 3 shows typical spectra produced by the mini-pole undulators.

We are going to reconstruct the front ends of BL01, BL05 and BL15, and to fabricate the prototype of new quadrupole magnets in FY2002.

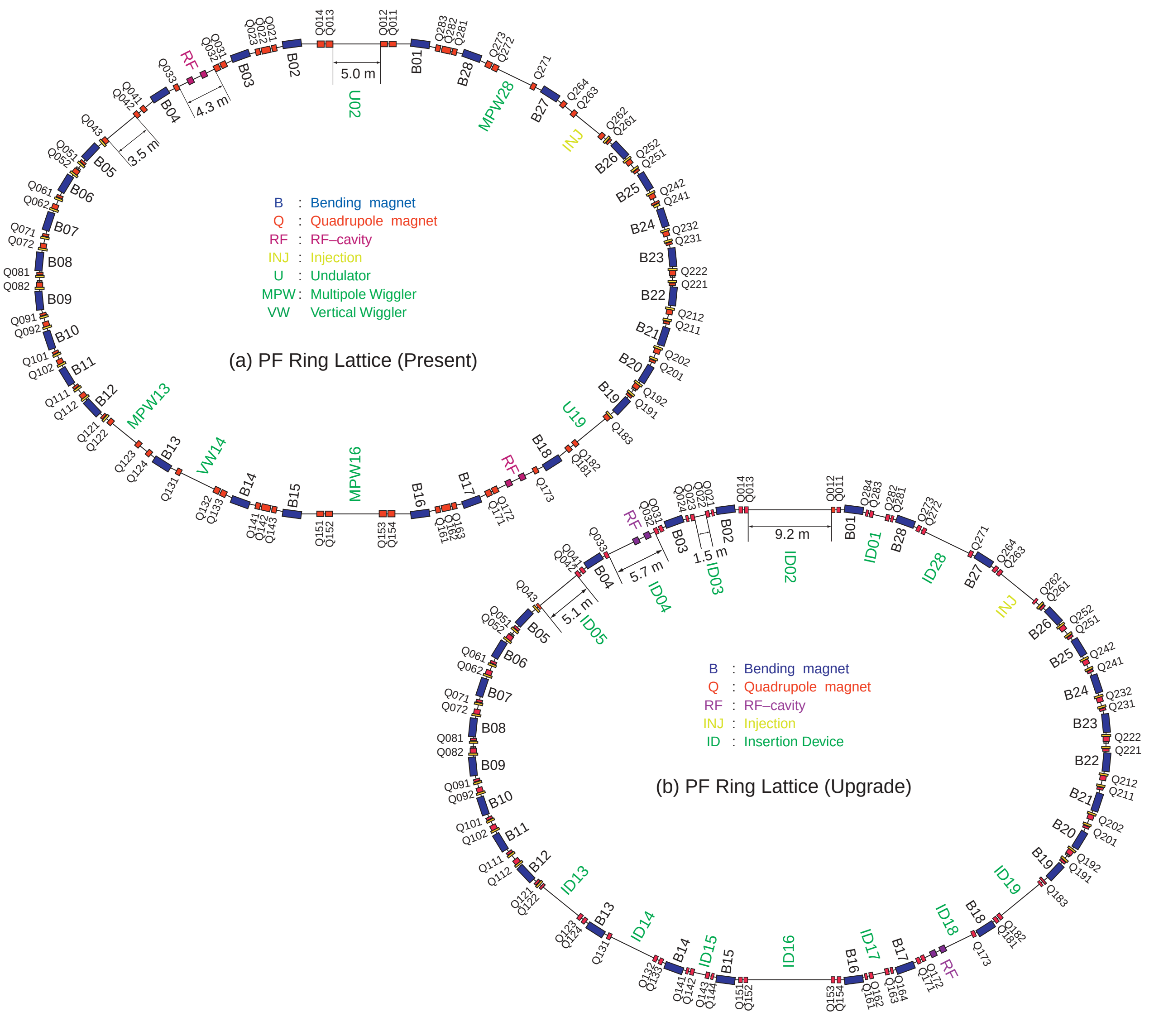

Figure 1
Lattice configurations of the PF Storage Ring; (a) present lattice and (b) upgraded lattice.

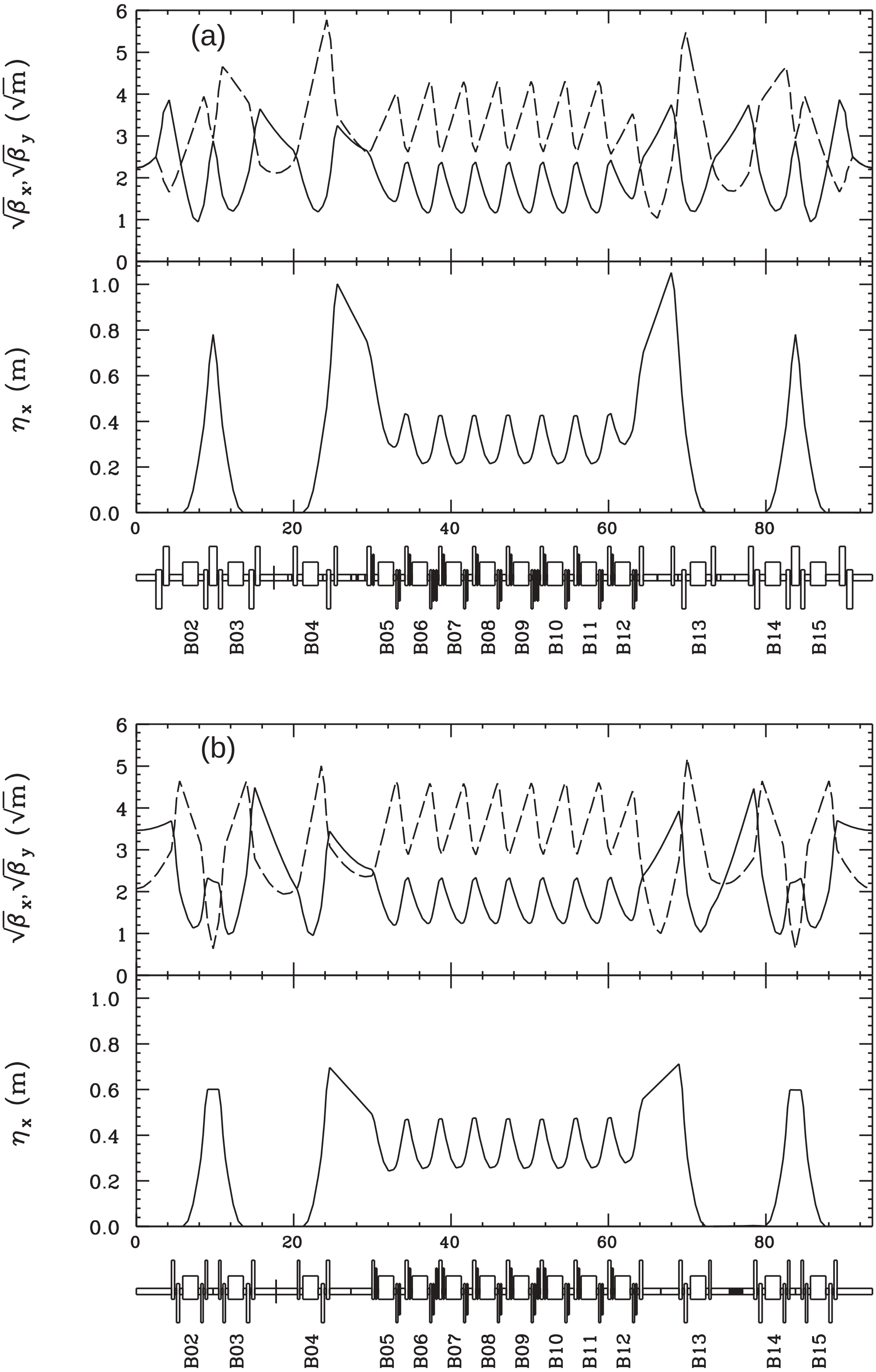

Figure 2
Optical functions in the half of the ring; (a) present one and (b) upgraded one. Top views show the root of beta function and bottom views show horizontal dispersion function. In the top views, the solid and dashed lines indicate the root of horizontal and vertical beta function, respectively.

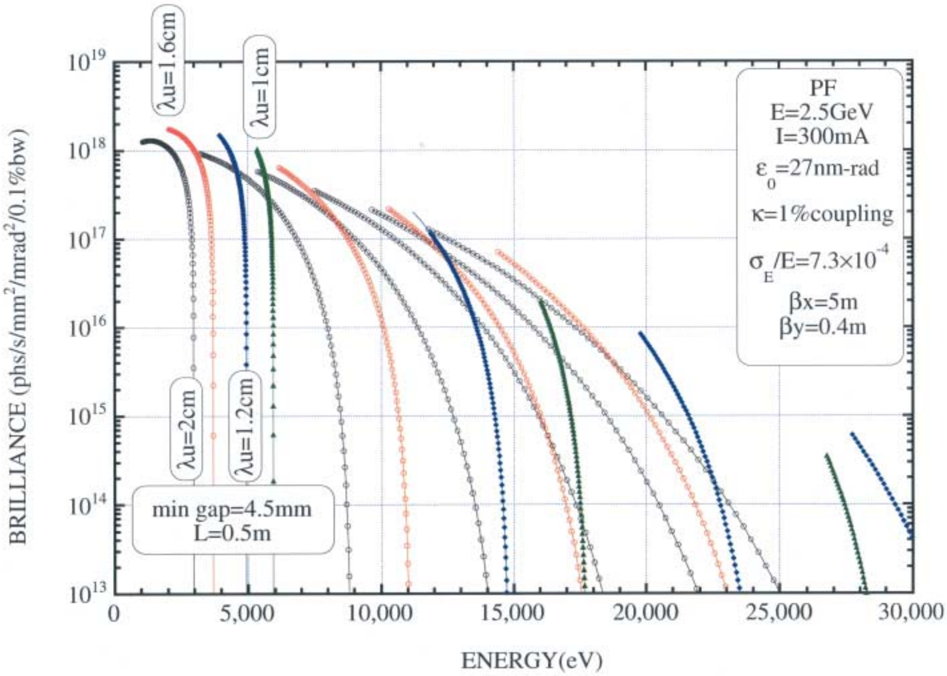

Figure 3
Typical spectra produced by the mini-pole undulators with a narrower gap.

4 Specifications of the Accelerators

Table 1 General parameters of the PF Storage Ring.

Energy		2.5 GeV	(max 3.0 GeV)
Initial stored current	multi-bunch	450 mA	(max 500 mA at 2.5 GeV)
	single bunch	70 mA	(max 100 mA)
Emittance	horizontal	36 nm-rad	
	vertical	~0.4 nm-rad	
Circumference		187 m	(bending radius = 8.66 m)
RF frequency		500.1 MHz	
Harmonic number		312	
Injection		2.5-GeV Linac	(electron/positron)
Beam lifetime		50 h (at 400 mA)	$I\tau \geq$ 20 Ah (at 400 mA)
Average vacuum pressure		$\leq 2 \times 10^{-8}$ Pa (at 300 mA)	
		P/I 6-7 $\times 10^{-8}$ Pa (at 300 mA)	
		~9 $\times 10^{-9}$ Pa (at 0 mA)	
Insertion devices	VW#14	Superconducting vertical wigger 5 T	
	U#02	60 period undulator K = 2.3~0.1	
	MPW#16	26 period multipole wigger/undulator 1.5~0.04 T	
	Revolver#19	Four way revolver-type undulator	
	MPW#13	13 period multipole wigger/undulator	
	EMPW#28	Elliptically polarized multipole wigger/helical undulator	
SR channels		SR experiment 22	
		Beam diagnosis 3	

Table 2 Beam parameters.

Horizontal tune	ν_x	9.60
Vertical tune	ν_y	4.28
Momentum compaction factor	α	0.0061
Natural chromaticity	ξ_x	−12.5
	ξ_y	−12.3
Bunch length	σ_z	1.0 cm
Damping time	transverse	7.8 ms
	longitudinal	3.9 ms
Energy spread		7.3×10^{-4}
Radiation loss		400 keV

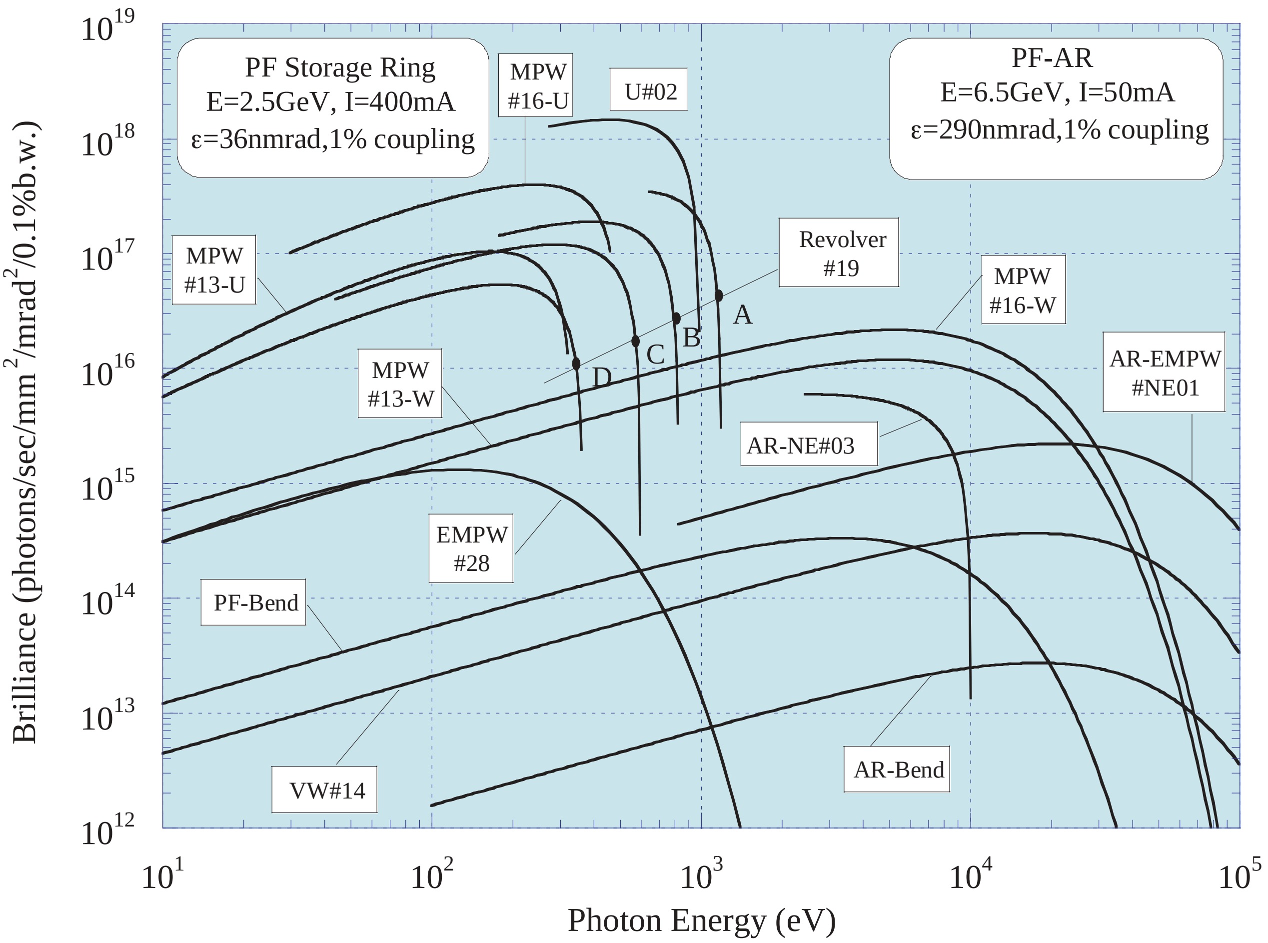

Figure 1
Synchrotron radiation spectra of the PF Storage Ring (2.5 GeV) and the PF-AR (6.5 GeV).
Brilliance of radiation vs. photon energy for the insertion devices (U#02, MPW#13, VW#14, MPW#16, Revolver#19 and EMPW#28) and the bending magnet (Bend) of the PF Storage Ring, and for the insertion device (EMPW#NE1 and UNE3) of the PF-AR. The name of each source of the PF Storage Ring is assigned in Table 3. Several insertion devices have both undulator and wiggler modes, which are denoted by U or W, respectively. The spectral curve of each undulator (or undulator mode of multipole wiggler) is a locus of the peak of the first harmonic within the allowable range of K-parameter. Spectra of Revolver#19 are shown for four kinds of period.

Table 3 Insertion devices

Calculated spectral performances of the bend source and 6 insertion devices at the PF Storage Ring (2.5 GeV, 400 mA) and the PF-AR (6.5 GeV, 50 mA). λ_u: period length, N: number of the periods, L: length of undulator or wiggler, $G_y(G_x)$: minimum vertical (horizontal) gap height, $B_y(B_x)$: maximum vertical (horizontal) magnetic field, Type of magnet, H: hybrid configuration, S.C.: super conducting magnet, σ_x,σ_y: horizontal or vertical beam size, σ_x',σ_y': horizontal or vertical beam divergence, $K_y(K_x)$: Vertical (horizontal) deflection parameter,
$\varepsilon_1/\varepsilon_0$: photon energy of the first harmonic (critical energy in the case of bend source or wiggler), D: photon flux density (photons/s/mrad^2/0.1%b.w.), B: brilliance (photons/s/mm^2/mrad^2/0.1%b.w.), P_T: total radiated power, $dP/d\Omega$: power in unit solid angle. Different operating modes of undulator and wiggler are denoted by -U and -W, respectively.

Name	λ_u cm	N	L m	$G_y(G_x)$ cm	$B_y(B_x)$ T	Type of magnet	σ_x mm	σ_y mm	σ'_x mrad	σ'_y mrad	$K_y(K_x)$	$\varepsilon_1/\varepsilon_c$ keV	D	B	P_T kW	$dP/d\Omega$ kW/mrad^2
PF Storage Ring																
Bend					0.96		0.39	0.059	0.186	0.013		4	4.80E+13	3.31E+14		0.081
U#02	6	60	3.6	2.8	0.4	H(NdFeB)	0.42	0.042	0.084	0.008	2.3	0.27	1.48E+17	1.28E+18	0.95	3.93
MPW#13-W	18	13	2.5	2.7	1.5	H(NdFeB)	0.86	0.019	0.117	0.018	25	6.2	1.29E+15	1.18E+16	8.64	3.38
MPW#13-U											2	0.108	1.08E+16	9.25E+16	0.055	0.25
VW#14				5	5	S.C.	0.58	0.036	0.083	0.01		20.8	4.84E+13	3.67E+14		0.42
MPW#16-W	12	26	3.12	1.9	1.5	H(NdFeB)	0.42	0.042	0.084	0.008	16.8	6.2	1.03E+15	8.95E+15	10.89	6.46
MPW#16-U											2	0.163	4.23E+16	3.63E+17	0.16	0.74
Revolver#19	5	46	2.3	3	0.28	H(NdFeB)	0.85	0.056	0.088	0.008	1.3	0.639	1.05E+17	3.47E+17	0.28	1.89
	7.2	32			0.4	H(NdFeB)					2.7	0.176	4.39E+16	1.44E+17	0.56	1.92
	10	23			0.54	H(NdFeB)					5	0.0437	1.28E+16	4.01E+16	1.02	2.02
	16.4	14			0.62	P(NdFeB)					9.5	0.0078	1.71E+15	4.29E+15	1.35	1.41
EMPW#28-W	16	12	1.92	3(11)	1(0.2)	P(NdFeB)	0.58	0.036	0.083	0.01	15(3)	4.1(90%)	3.07E+14	2.28E+15	2.84	0.46
EMPW#28-U											3(3)	0.182(99%)	1.81E+16	1.33E+17	0.03	0.087
PF-AR																
Bend							1	0.2	0.593	0.036		26	3.25E+13	2.59E+13		0.34
EMPW#NE1W	16	21	3.36	3(11)	0.94	P(NdFeB)	1.07	1.07	0.268	0.032	15(3)	28(90%)	1.53E+15	2.12E+15	4.6	17.7
EMPW#NE1U					1(0.2)						3(3)	0.25(97%)	3.41E+15	4.70E+15	0.35	0.77
U#NE3	4	90	3.6	1	0.8	P(NdFeB)	1.57	0.17	0.312	0.029	3	1.8	1.01E+16	6.01E+16	3.09	25.7
U#NW2	4	90	3.6	1	0.8	P(NdFeB)	1.57	0.17	0.312	0.029	3	1.8	1.01E+16	6.01E+16	3.09	25.7

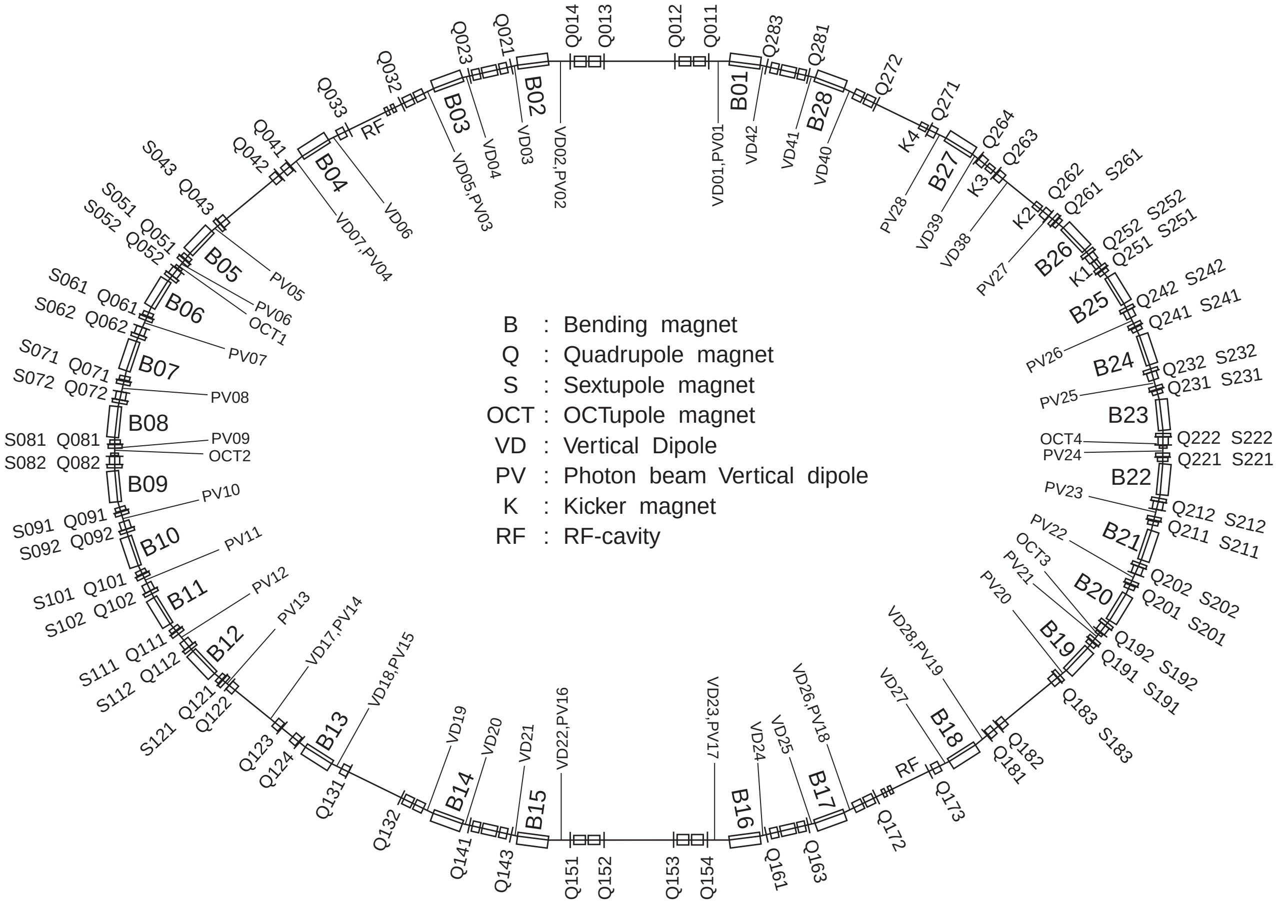

Figure 2
Ring lattice components.

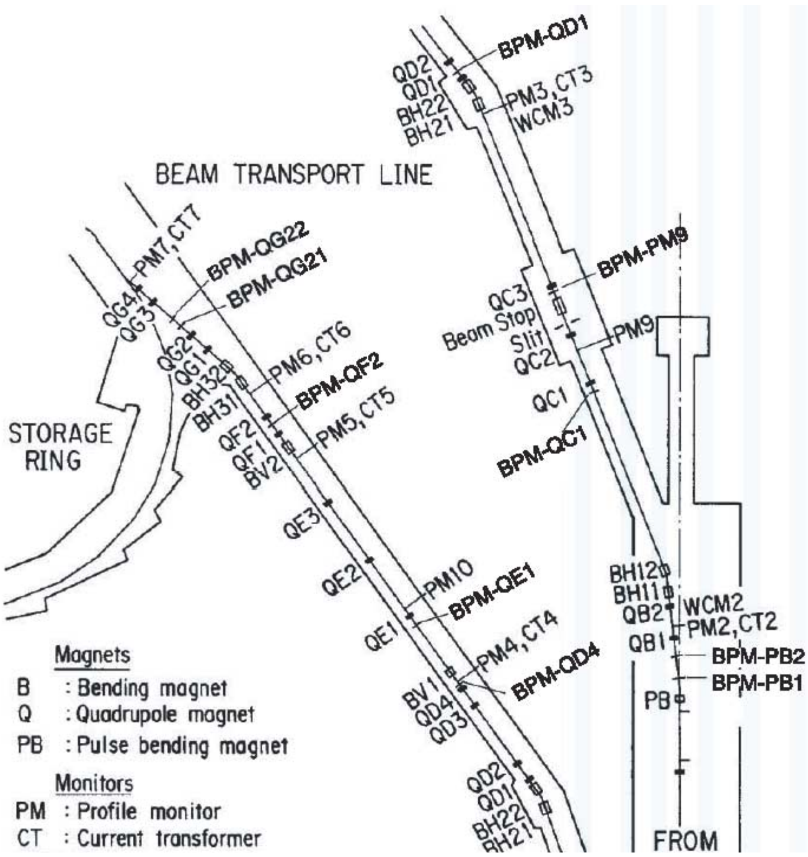

Figure 3
Beam-transport line.